23rd ABCM International Congress of Mechanical Engineering
December 6-11, 2015, Rio de Janeiro, RJ, Brazil

# FATIGUE CRACK GROWTH BEHAVIOR IN THE BASE METAL 90° AND 180° FROM THE WELDED JOINT OF AN API 5L X-70 PIPELINE STEEL

**Vitor Scarabeli Barbosa**[1]
scarabeli.v@gmail.com

**Bruno Antonio Sorrija**[1]
sorrija.bruno@gmail.com

**Marcelino Pereira do Nascimento**[1]
pereira@feg.unesp.br

UNESP – Univ. Estadual Paulista, DMT – Department of Materials and Technology, Av. Ariberto Pereira da Cunha, 333, Guaratinguetá, SP, 12.516-410, Brazil.

***Abstract.*** *The aim of this paper is investigate how the UOE process may influence the fatigue crack growth (FCG) rates of an API 5L X70 PSL2, High Strength Low Alloy (HSLA) steel pipe. The fatigue crack growth rate test parameters and the geometry of the Compact Tension (CT) specimens were both in accordance to the ASTM E647 standard. Specimens had been machined from pipe samples taken from 90º and 180º of the longitudinal welded joint, and the Paris-Erdogan Law has been used to determine the fatigue crack growth parameters C and m for both, 90º and 180º positions. The results of the fatigue crack growth rate tests showed significant differences between regions situated 90º and 180º of the welded joint region, which can be potentially related to the steel pipe manufacturing process.*

***Keywords:*** *UOE process, API 5L X70, Paris-Erdogan law, fatigue crack growth rate*

## 1. INTRODUCTION

The growing demand for energy resources has driven oil and natural gas exploration to harsh environments, especially to ultra-deep water (Karampour *et al*., 2013; Mohtadi-Bonab *et al*., 2013), and according to Karampour *et al*. (2013) it is estimated that approximately one-quarter of the offshore oil production will be in deep water by 2015. Concerning Brazilian oil and gas industry, in the current scenario most of the country hydrocarbons come from offshore wells, including the ultra-deep water Basin Pre-salt reservoirs. Brazilian National Agency of Petroleum, Natural Gas and Biofuels (ANP), which regulates the oil market in Brazil, provides some important perspectives on country oil and gas exploration. According to the data available in the ANP Biofuels Statistical Yearbook, Brazil had 15.6 billion barrels of proved oil reserves as of December 31, 2013, of which over 94% are located offshore. Following a similar trend, almost 85% of the 458 million cubic meters of proved natural gas reserves are located on the seabed (ANP, 2014).

Transporting both unprocessed and processed oil and gas (as well other fluids like lift gases) in deep and ultra-deep water environment requires long offshore pipes and consequently the design of such structures poses many engineering challenges that must take into account (COFS, 2012; Karampour *et al*., 2013). Offshore structural components such as linepipes for oil and gas exploration are invariably exposed to some type of cyclic loads, which can result in high rates of fatigue damage (Beden *et al*., 2012; Beltrão *et al*., 2011). These dynamic loads comes from sources like waves, (including those loads caused by slamming and variable pressures) and specially ocean flow currents, which can lead to high frequency vibration of the riser pipe due to vortex shedding (Bay 2001; DNV, 2003; Gerwick, 2007).

Although the X80 linepipeline steel has become the state of the art for high pressure gas pipeline, the X70 (also known as Grade 485) linepipe steel is still widely employed in the world (Jiang and Chen, 2012). API X70 grade linepipe steels are formed from individual plates which are shaped into pipes (Sohn *et al*., 2013). Large diameter and thick wall linepipes, used in both deep and ultra-deepwater operations, are usually manufactured by the UOE method (Chatzopoulou *et al*., 2014; Herynk *et al*., 2007; Zhao *et al*., 2013). In this process, the hot-rolled plate edges are first crimped into circular arcs, then formed into an U-shape in the "U-press", and finally pressed into a circular shape in the "O-press". After forming the pipe is welded by submerged arc welding, with subsequent mechanical expansion through a hydraulic mandrel, longitudinally positioned inside the welded pipe, in order to improve its circularity (Herynk *et al*., 2007; Toscano, 2009; Wen *et al*., 2001; Yang *et al*., 2008). The forming process accentuates the differences between outer and inner walls properties of pipes due different strains, i.e., tensile strains on the outer wall and compressive strains on the inner wall. In addition, the manufacturing steps of UOE process also introduce some variation in properties around the circumference (Sohn *et al*., 2013, Kyriakides and Corona, 2007).

Raffo et al. (2007) developed 2D finite element model to simulate the UOE process in order to analyze the influence of each stage of the process on the material plastic deformations and residual stresses. As can be seen from Raffo *et al*. (2007) work, in fact, the UOE process induces a significant gradient strains around the pipe's circumference.

Historical data have shown that fatigue damage contributes to approximately 90% of all mechanical service failures (Campbell, 2008). Oil and gas transmission linepipes have proved a good operational reliability (Cosham and Hopkins, 2002). However, like any engineering structure subjected to cyclic loading, linepipes can occasionally fail and fatigue failure is the most common form of linepipe failure (Arora, *et al*., 2013; Beden, *et al*., 2012; Cosham and Hopkins, 2002). In a particular case of cyclic loading, the crack grows under a characteristic behavior called fatigue crack growth (Dowling, 2007).

Modern defect-tolerant design approaches based on fracture mechanics concepts such as leak-before-break, which is widely used in structural integrity design of pressure vessel and pipe, has been the subject of many scientific investigations. The linear elastic fracture mechanics (LEFM) concepts provides a rational basis for establishing flaw tolerance limits (Anderson, 2005).

The service life or inspection intervals can be estimated from assessment the crack growth behavior under specific loading conditions and service environment (Campbell, 2008). Under (LEFM) conditions, fatigue crack growth rate can be characterized by the stress-intensity factor (Anderson, 2005; Campbell, 2008).

Fatigue crack growth rate behavior in high strength low alloy (HSLA) linepipe steels has been a subject of intense research (Beltrão, *et al*., 2007; Beltrão, *et al*., 2011; Li, *et al*., 2014). However, there are very few studies that investigate the influence of UOE process on fatigue properties.

The aim of this paper is investigate how the UOE process can affect the fatigue crack growth rate. For this purpose, two specimens had been machined from pipe samples taken from 90º and 180º of the longitudinal welded joint. Results of fatigue crack propagation experiments were plotted on a log-log graph that relates fatigue crack growth rate (da/dN) as a function of crack-tip stress-intensity factor range (ΔK), as can be seen in Figure 1. This typical experimental curve is characterized by three stages which are generally designated to as stage I, II and III respectively. The prediction of fatigue crack growth rates were based on Paris law (Paris and Erdogan, 1963).

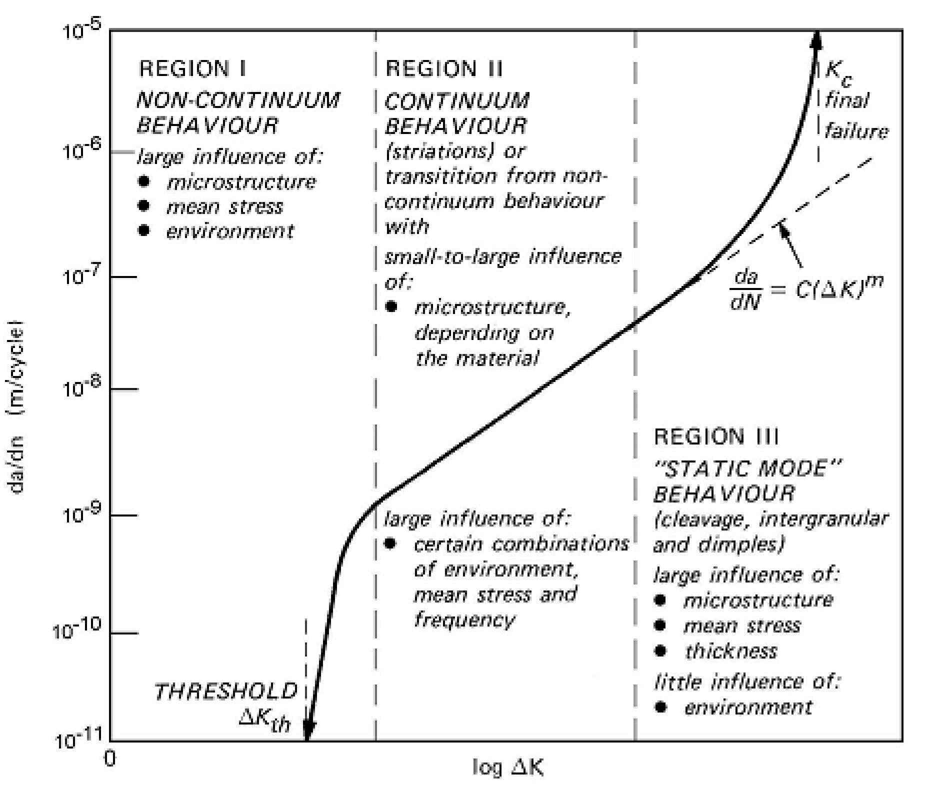


Figure 1. A typical fatigue crack growth rate experimental curve (JANSSEN, *et al*., 2004).

## 2. TEST MATERIAL AND EXPERIMENTAL PROCEDURE

### 2.1 Material

The material used in this study was obtained from an API 5L grade X70[1] pipe (used for oil and gas transportation) with 700 mm outside diameter and 15.9 mm wall thickness formed by UOE-SAWL (Submerged Arc-welding Longitudinal) process. The chemical composition (mass %, determined by optical emission spectroscopy - OES) of API 5L X-70 grade steel and the specification according to the American Petroleum Institute's (API) standard 5L are shown in Table 1.

Table 1. Chemical composition of API 5L X-70 grade steel specified by API 5L.

| Steel Grade | Mass fraction, based upon heat and product analyses % maximum | | | | | | | | | Carbon equivalent % maximum |
|---|---|---|---|---|---|---|---|---|---|---|
| | C | Si | Mn | P | S | V | Nb | Ti | Other | Pcm |
| API 5L X70 | 0.12 | 0.45 | 1.70 | 0.025 | 0.015 | [a] | [a] | [a] | [b] | 0.25 |
| DNV-0S SMYS 485 | 0.12 | 0.45 | 1.75 | 0.020 | 0.010 | 0.10 [a] | 0.08 [a] | 0.06 [a] | [b] | 0.22 |
| Experimental 5L X70 | 0.10 | 0.16 | 1.34 | 0.008 | 0.0013 | 0.059 | 0.0505 | 0.0078 | matched | 0.1984 |

[a] The sum of the Nb, V, and Ti contents shall be ≤ 0.15%. [b] Cu ≤ 0.50%; Ni ≤ 0.50%; Cr ≤ 0.50%; Mo ≤ 0.50%.

As can be seen from Tab. 1, all alloy elements had measured values below (or close to) the maximum values set by API standard code.

### 2.2 Material microstructure

The standard metallographic analysis of API X70 steel was carried out through sectioning and cutting, mounting, planar grinding, rough polishing, final polishing, and etching of two samples in 2% nital solution in order to reveal their microstructures. For metallographic examination, two specimens of the base metal were removed from the pipe. One from the longitudinal and one from the transverse section were removed with respect to the rolling direction. Both base metal samples were taken from 180° position of the pipe body. The characterization and classification of the various ferritic microstructures of base metal was based on ferritic classification system proposed by Bainite Committee of ISIJ.

### 2.3 Tensile tests

For mechanical property evaluation, tensile test has been performed in transverse direction to the axis of the pipeline as suggested by API 5L standard (API, 2008). Due to the dimensional characteristics of the pipe (Ø 27 ½" x 5/8" wall thickness), subsized tensile specimens were machined with 25 mm gauge length and 6.25 mm gauge diameter (as per ASTM A 370) as indicated in Figs. 2(a) and 2(b). Tensile tests were carried out on a 100 kN capacity Instron 8801 servo hydraulic testing machine. All tests were performed under low displacement rate of 1 mm/min at room temperature. Tensile test specimens were taken from the 90° and 180° position.

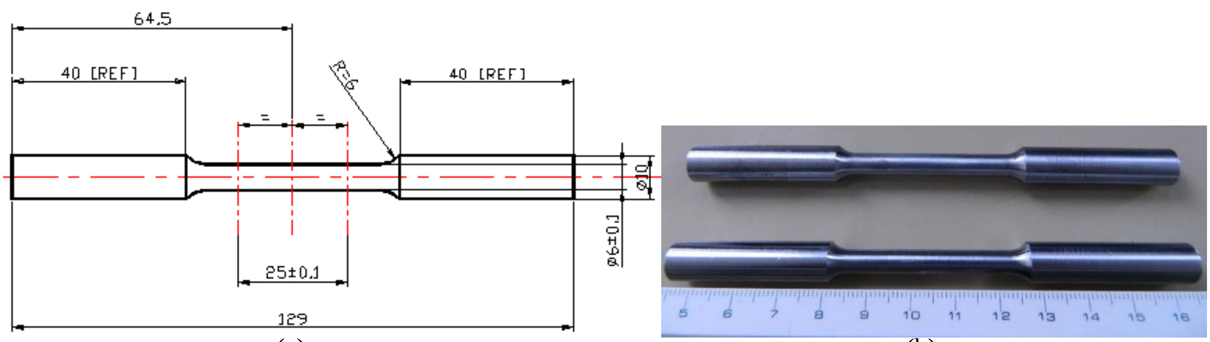


(a) (b)

Figure 2. Schematic illustration: (a) geometry and dimensions of sub-size tensile specimens; (b) sub-size tensile specimens employed in the experiments.

[1] The API X70 pipe has a minimum specified yield strength of 485 MPa and ultimate tensile strength of 570 MPa, according to API 5L specifications.

### 2.4 Fatigue crack propagation tests

Fatigue crack growth tests in standard compact-type C(T) specimens were carried out in the base metal machined from 90° and 180° at the welded joint as shown in Figure 3(a). The dimensions and configuration of C(T) specimens according to the ASTM E399-12 are shown in Figure 3(b). All C(T) specimens were machined C-L orientation, according to ASTM standard procedure E399-12, (where C is the circumferential and L is the longitudinal direction). It should be point out that, all C(T) specimens were taken from the same pipe ring.

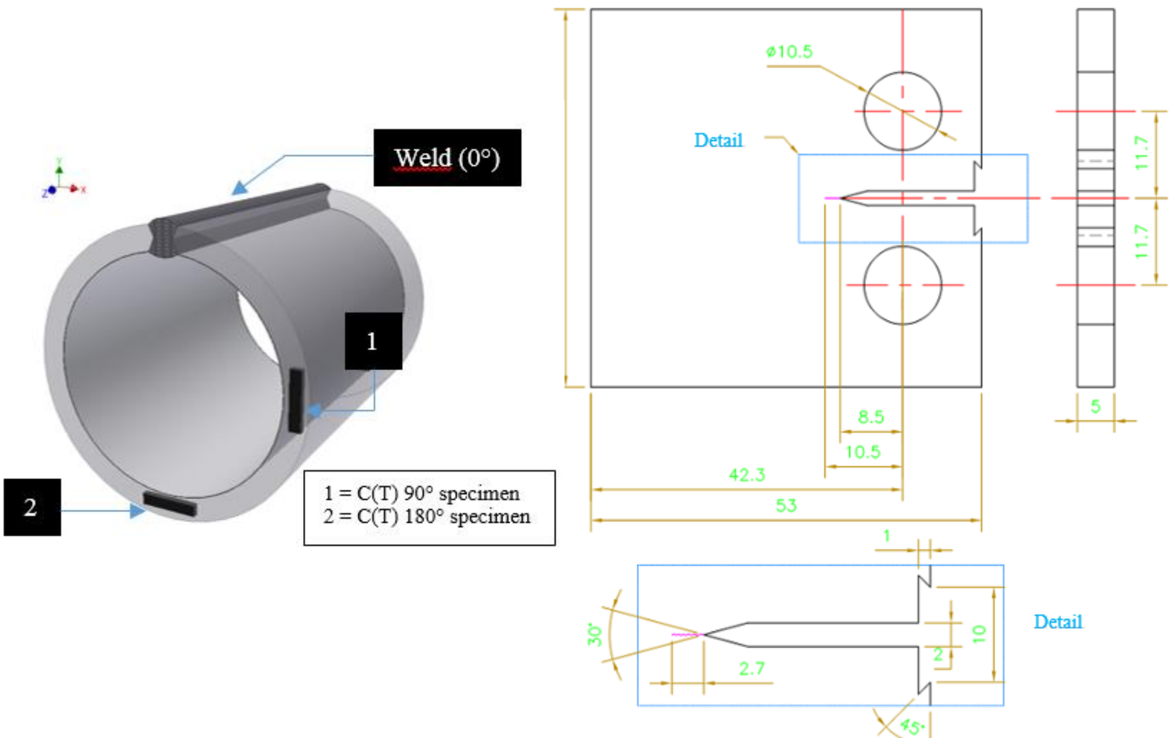


(a) (b)

Figure 3. (a) Location and orientation of the fatigue crack growth rate testing (out of scale); (b) standard compact C(T) specimen dimension (mm).

Following machining by electro-discharge, the specimens have been precracked under fatigue loading using sinusoidal waveform at room temperature in an Instron model 8801 servo hydraulic testing machine according to ASTM E647-08 guideline. After the precracking, the fatigue crack growth tests have been carried out in atmospheric air and room temperature in the same machine. The fatigue crack growth tests were in accordance to ASTM E647, and have been carried out under constant amplitude cyclic loading with a sinusoidal wave form at a frequency of 10 Hz, a load ratio ($R = P_{min}/P_{\max}$) of 0.1 and a load range $\Delta P$ = 8.1 kN. The crack length measurement was monitored by the compliance technique employing a back face strain gauge extensometer with a 10 mm gauge length. The resulting fatigue crack growth data were reported by means of *a-N* graph and FCG rate *da/dN* was represented graphically as a function of the stress-intensity factor range, ΔK, to determine the Paris Law constants, *i.e.*, crack growth rate parameters C and m. According to the ASTM E647-08 standard for C(T) specimens, the stress-intensity factor range (ΔK), which is calculated from expressions based on linear elastic stress analysis at the crack tip, can be determined from the following expression:

$$\Delta K = \frac{\Delta P}{B.\sqrt{W}} \frac{(2+\alpha)}{(1-\alpha)^{3/2}} \left(0.886 + 4.64\alpha - 13.32\alpha^2 + 14.72\alpha^3 - 5.6\alpha^4\right) \quad (1)$$

where, ΔP is the load range, B the specimen thickness, W the distance between point of load application and free boundary [see Fig. 3(b)], and α= a/W, which is valid for a/W ≥ 0.2.

## 3. RESULTS AND DISCUSSIONS

### 3.1 Material microstructure

Figures 4(a) and 4(b) shows the microstructure on the longitudinal and transverse direction in relation to the rolling direction, respectively.

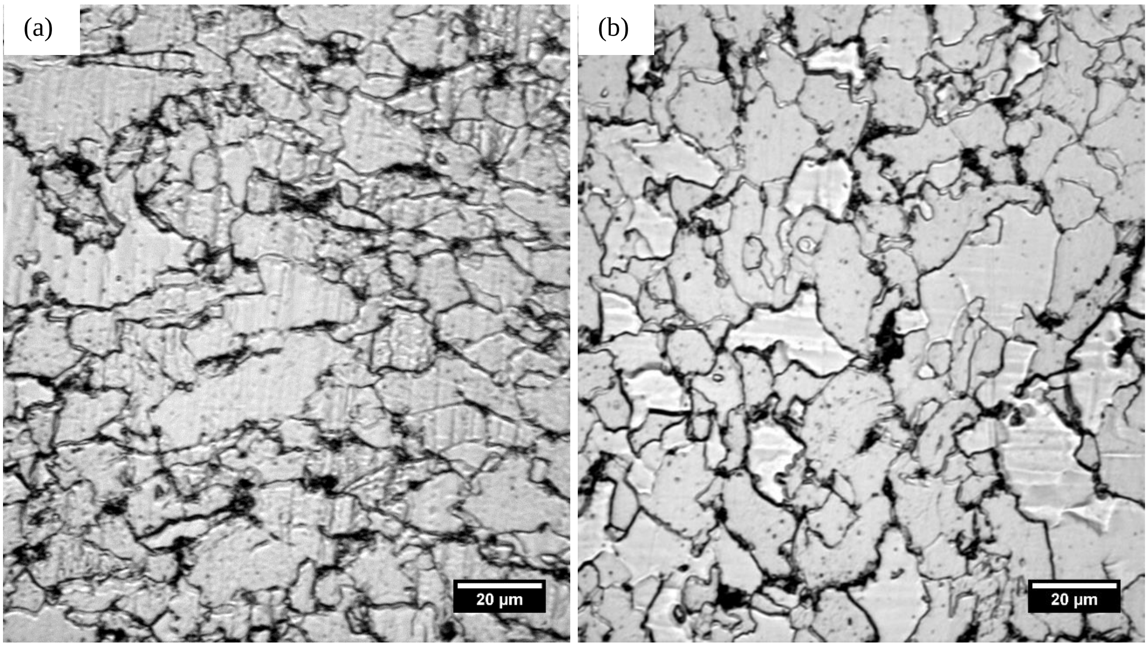


Figure 4. Microstructure of the API 5L X70 pipeline steel: (a) longitudinal section (500x) (b) transverse section (500x).

From the observation by optical microscope, the microstructure of the API X70 linepipe steel is essentially composed by typical ferritic-pearlitic microstructure of normalized steel. Note also that the ferrite forms with a variety of morphologies. According to system proposed by Bainite Committee of ISIJ (Araki, *et al.*, 1992), the ferrite morphologies shown in Figure 4 consists of polygonal ferrite (PF) and quasi-polygonal ferrite (QF). In addition, it can be noticed that the microstructure is dominated by ferrite phase due to a low carbon content, as can be seen from Table 1. According to Krauss (2005), the PF grains have equiaxed and continuous boundaries, and the QF grains have irregular and jagged boundaries.

### 3.2 Tensile tests

The mechanical properties of API X70 steel obtained from pipeline transverse specimens, in accordance with ASTM A 370, are set out in Table 2. As can be seen from this data, according to the specification of API 5L 44$^{th}$, all the specimens tested in present study satisfy the requirement of X70 grade pipeline.

Table 2. Room-temperature tensile properties of API 5L X70 steel in the transverse direction.

| Pipe grade | Tensile properties | | | | | | | | | |
|---|---|---|---|---|---|---|---|---|---|---|
| | Yield Strength (YS) [MPa] | | | | Tensile Strength (TS) [MPa] | | | | Yield Ratio (YS/TS) | |
| L485Q or X70Q<br>L485M or X70M | 180° | | 90° | | 180° | | 90° | | 180° | 90° |
| | Min. | Max. | Min. | Max. | Min. | Max. | Min. | Max. | Max. | Max. |
| | 485 | 635 | (c) | (c) | 570 | 760 | (c) | (c) | 0.93 | (c) |
| Specimen 1 | 553.78 | | 498.54 | | 608.81 | | 554.65 | | 0.90 | 0.90 |
| Specimen 2 | 563.46 | | 500.95 | | 613.83 | | 566.40 | | 0.91 | 0.88 |
| Specimen 3 | 558.46 | | 502.98 | | 610.80 | | 559.64 | | 0.91 | 0.90 |
| Mean values | 558.57 | | 500.82 | | 611.15 | | 560.23 | | 0.91 | 0.89 |
| Standard deviation | 4.84 | | 2.22 | | 2.53 | | 5.90 | | 0.01 | 0.01 |

(c) The requirements for the results of tensile tests for specimens taken longitudinally from the pipe body 90° from the seam weld are not specified by API Specification 5L.

### 3.3 FCP Tests

Figure 5 shows the fatigue crack growth as a function of number of cycles (N) for the base metal 90° and base metal 180°. According to the results, it can be noticed that there is a clear difference between crack growth when both positions are compared. The specimens, which had been taken from the 180 ° position, have endured around 25% more cycles before the fracture when compared to the specimens taken from the 90º position.

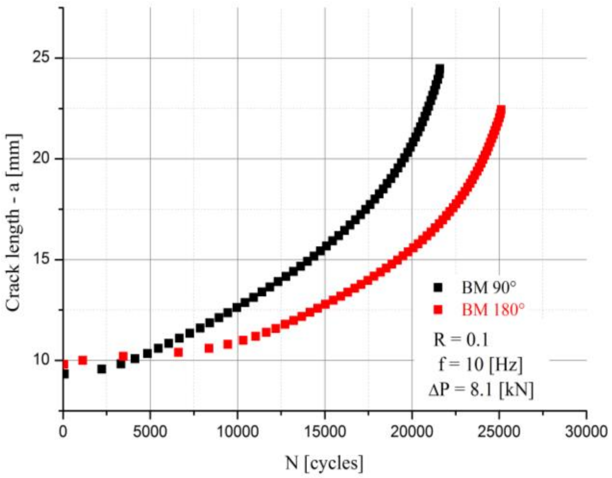


Figure 5. Crack length (a) as a function of cycles (N).

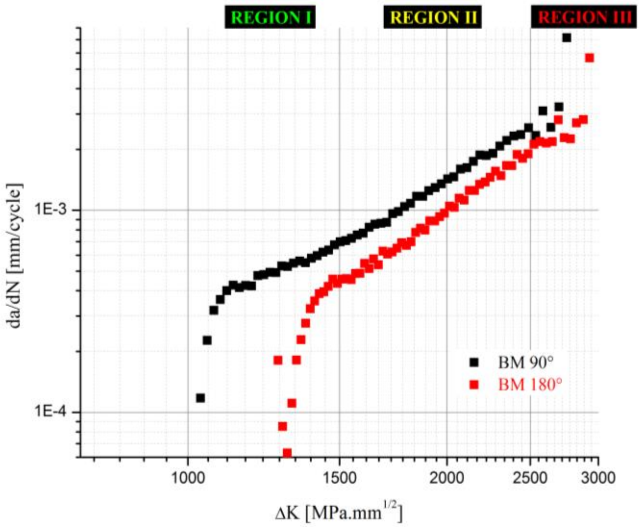


Figure 6. Fatigue crack growth rates curves.

The experimental data of da/dN versus ΔK are show in Figure 6. Concerning fatigue crack growth rates curves, there are also noticeable differences between both positions for all the three stages of the crack growth rate. As can be seen in Figure 6, the stress intensity near threshold ($\Delta K_{th}$), which is at the lower end of the ΔK range, is well distinguished. The threshold region defines a critical stress intensity below which fatigue crack growth is not detectable. Concerning Region I, it is noticed that specimens taken from the 180º position showed a tendency towards higher value of $\Delta K_{th}$, when compared to the specimens taken from the 90º position. In the mid-region of stress intensities (Region II) for both positions, the log da/dN versus log ΔK curve show an essentially linear and stable behavior. The stress intensities data of region II were modeled according to the Paris Law (Paris and Erdogan, 1963), where the FCG rate, da/dN, is described in terms of the stress intensity range ΔK according to the following relationship:

$$\frac{da}{dN} = C(\Delta K)^m \qquad (2)$$

where C and m are experimental values obtained from fitting curve.

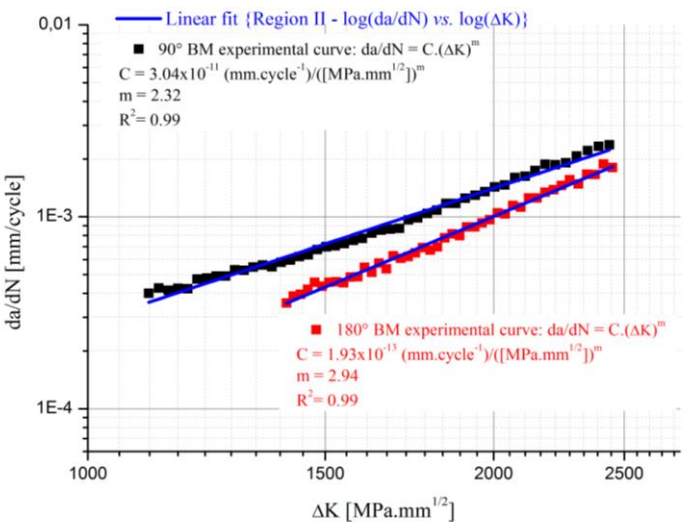


Figure 7. Fitting of mid-region (region II) with a Paris law.

Using the results of Figure 7, when Region II is analyzed, it can be noticed that specimens taken from the 180º exhibits a higher value of m, which would suggest that a crack should grow faster in this position when it is compared to the 90º position. However, the parameter C is two orders of magnitude lower for the 180º position which may compensate its highest value of m. It should be emphasized that the steady state region (stage II) of fatigue crack growth is one of the most important parameter in damage tolerant design philosophy (Ribeiro *et al.*, 2005). Furthermore, the results show a tendency of the crack growth rate dependency upon the difference between mechanical properties of different locations around the pipe circumference. In this case, the tensile test specimens and C(T) specimen taken from the pipe body 90° from the seam weld show low yield stress and the higher FCG rate, respectively. Such an approach, however, it requires a more detailed study to investigate the influence of variations in mechanical properties around the circumference of the tube on the fatigue crack growth rates.

In complement, it can be noticed that there is a good fit between the test curves and the linear fit, with a value of $R^2$ of 0.99 for the 90º position specimen and of 0.99 for the specimen taken from the 180º position. As the crack advances and enters in Region III, it can be noticed that the values of $\Delta Kc$ is slightly higher for the 90º position, thus the specimens which had been taken from this position have failed some cycles before the ones that had been taken from 180º position.

## 4. CONCLUSIONS

In this work, a study of crack growth rate in different positions of an APIL 5L X70 steel pipe has been made. According to obtained results, it can be noticed that there are significant differences between the crack growth rates between samples taken from 90° and 180º from the welded joint. Differences in the $\Delta K$ near threshold and $\Delta Kc$ values, when 90º and 180º positions are compared, suggest that the UOE process impacts in the fatigue properties of the steel plates. The base metal 90° position initially presented the highest fatigue crack growth rate. However, at higher $\Delta K$ values both metal pipe positions show similar fatigue behavior. For this, a fatigue fracture is expected to happen early in the 90º position, which is much more affected by the UOE forming, when it is compared to the 180º position, which in terms of strain is much closer than the base material. However, it can be noticed that the values of m for the 180º position are higher than the ones observed in the 90º position. This suggests that a crack will grow faster in the 180º position, and this should lead to a fracture before the 90º position, due the power law nature of the Paris-Erdogan equation. Although, the values of C are two orders of magnitude lower for the 180º position, which apparently compensate its higher values of m.

## 5. ACKNOWLEDGMENTS

The authors are grateful to CAPES and FAPESP (Processes No. 2008/56424-5 and 2010/02291-4) for financial support.

## 6. REFERENCES

Anderson, T.L., 2005. “Fracture mechanics: Fundamentals and applications”. CRC Press, Florida, 3rd edition.

ANP, 2014. “Oil, Natural Gas, and Biofuels Statistical Yearbook 2014” Agência Nacional do Petróleo, Gás Natural e Biocombustíveis. 25 May. 2015 < http://www.anp.gov.br>.

API 5L, 2008. “Specification for line pipe steel API5L”. American Petroleum Institute, 44th edition, Washington D.C.

Araki, T., Kozasu, I., Tankechi, H., Shibata, K., Enomoto, M. and Tamehiro, H., 1992. “Atlas for Bainitic Microstructures”, *Iron and Steel Institute of Japan*, vol. 1, Japan.

Arora, P., Singh, P.K., Bhasin, V., Vaze, K.K., Pukazhendhi, D.M., Gandhi, P. and Raghava, G., 2013. “Fatigue crack growth behavior in pies and elbows of carbon steel and stainless steel materials”. *Procedia Engineering*, Vol. 55, p. 703-709.

ASTM A370, 2014. “Standard Test Methods and Definitions for Mechanical Testing of Steel Products”. American Society For Testing And Materials.

ASTM E399, 2012. “Test Method for Linear-Elastic Plane-Strain Fracture Toughness KIC of Metallic Materials”. American Society For Testing And Materials.

ASTM E647, 2013. “Standard Test Method for Measurement of Fatigue Crack Growth Rates”. American Society For Testing And Materials.

Bay, Y., 2001. “Fatigue of Risers”. In *Pipelines and Risers*. Vol. 3. Elsevier Ocean Engineering Book Series, Amsterdam, chap. 22, p. 413-431.

Beden, S.M., Abdullah, S. and Ariffin, A.K., 2012. “Fatigue crack growth rate of API X70 steel pipelines under spectrum loading”. *International Journal of Pressure Vessels and Piping*, Vol. 96-97, p. 7-12.

Beltrão, M.A.N., Marco Filho, F., Castrodeza, E. M. and Bastian, F. L., 2007. “Fatigue behavior of welded joints of API 5L X-65 and X-70 steels under variable amplitude loading”. *Soldagem & Inspeção*, Vol. 12, p. 133-140.

Beltrão, M.A.N., Castrodeza, E.M. and Bastian, F.L., 2011. "Fatigue crack propagation in API 5L X-70 pipeline steel longitudinal welded joints under constant and variable amplitudes". *Fatigue & Fracture of Engineering Materials & Structure*, Vol. 34, n. 5, p. 321-328.

Campbell, F.C., 2008. "Fatigue". In *Elements of Metallurgy and Engineering Alloys.* ASM International, Ohio, chap. 14, p. 243-264.

Chatzopoulou, G., Varelis, G.E. and Karamanos, S.A., 2014. "Finite element analysis of UOE pipes under external pressure and bending". In *Proceedings of the Twenty-fourth (2014) International Ocean and Polar Engineering Conference.* Busan, Korea.

COFS, 2012. "Subsea Pipelines Collaboration Cluster" Centre For Offshore Foundation Systems. 09 May. 2015 <http://www.cofs.uwa.edu.au/publications>.

Cosham, A. and Hopkins, P., 2002. "The pipeline defect assessment manual, IPC02-27067, Proceedings of IPC 2002". In *International Pipeline Conference, American Society of Mechanical Engineers,* Calgary, Alberta, Canada.

DNV OS-F101, 2013. "Submarine Pipeline Systems – Offshore Standard". Det Norske Veritas, Oslo, Norway.

DNV Software, 2003. "Fatigue Assessment Using SESAM Program Modules Stofat, Framework and Postresp A White Paper" Det Norske Veritas. 25 May. 2015 < http://www.dnv.pl/resources>.

Dowling, N.E., 2007. "Mechanical Behavior of Materials: Engineering Methods for Deformation, Fracture, and Fatigue". Pearson Prentice Hall, 3rd edition.

Gerwick, Jr.B.C., 2007. "Physical Environmental Aspects of Marine and Offshore Construction". In *Construction of Marine and Offshore Structures*. CRC Press, Boca Raton, 3rd edition, chap. 1, p. 15-47.

Herynk, M. D., Kyriakides, S., Onoufriou, A. and Yun, H.D., 2007. "Effects of the UOE/UOC pipe manufacturing processes on pipe collapse pressure". *International Journal of Mechanical Sciences*, Vol. 49, n. 5, p. 533-553.

Janssen, M., Zuidema, J. and Wanhill, R., 2004. "Fracture Mechanics"**.** Spon Press, New York, 2nd edition.

Jiang, Y. and Chen, M., 2012. "Researches on the Fatigue Crack Propagation of Pipeline Steel". *Energy Procedia*, Vol. 14, p. 524-528.

Karampour, H., Albermani, F. and Veidt, M., 2013. "Buckle interaction in deep subsea pipelines". *Thin-Walled Structures*, Vol. 72, p. 113-120.

Krauss, G., 2005. "Steels: processing, structure, and performance". Materials Park, Ohio: ASM International.

Kyriakides, S. and Corona, E., 2007. "Pipe and tube manufacturing processes". In *Mechanics of Offshore Pipelines*. Vol.1 Buckling and Collapse. Elsevier Science, 1st edition, chap.3, p. 59-88.

Li, L., Yang, Y. H., Xu, Z., Chen, G. and Chen, X., 2014. "Fatigue crack growth law of API X80 pipeline steel under various stress ratios based on J-integral". *Fatigue and Fracture of Engineering Materials and Structures*, Vol. 37, n. 10, p. 1124-1135.

Mohtadi-Bonab, M.A., Szpunar, J.A. and Razavi-Tousi, S.S., 2013. "A comparative study of hydrogen induced cracking behavior in API 5L X60 and X70 pipeline steels". *Engineering Failure Analysis*, Vol. 33, p. 163-175.

Paris, P.C. and Erdogan, F., 1963. "A critical analysis of crack propagation laws". *Journal of Basic Engineering*, Vol. 85, n. 4, p.528-534.

Raffo, J., Toscano, R.G., Mantovano, L. and Dvorkin, E., 2007. "Numerical model of UOE steel pipes: forming process and structural behavior". *Associación Argentina de Mecánica Computacional*, Vol. XXVI, p. 317-333.

Ribeiro, A.S., De Jesus, A.M.P. and Fernandes, A.A. , 2005. "Fatigue crack propagaiton rates of the aluminium alloy 6061-7651". In *Proceedings of the 18th International Congress of Mechanical Engineering – COBEM 2005*. Ouro Preto, Brazil.

Sohn, S.S., Han, S.Y., Bae, J-h., Kim, H.S. and Lee, S., 2013. "Effects of microstructure and pipe forming strain on yield strength before and after spiral pipe forming of API X70 and X80 linepipe steel sheets". *Materials Science & Engineering A*, Vol. 573, p. 18-26.

Toscano, R.G., 2009. *Collapse and post-collapse behavior of steel pipes under external pressure and bending. Application to deep water pipelines.* Ph.D. thesis, University of Buenos Aires, Buenos Aires.

Wen, S.W., Hilton, P. and Farrugia, D.C.J., 2001. "Finite element modelling of a submerged arc welding process". *Journal of Materials Processing Technology*, Vol. 119, n. 1, p. 203-209.

Yang, Z.Z., Tian, W., Ma, Q.R., Li, Y.L., Li, J.K., Gao, J.Z., Zhang, H.N. and YANG, Y.H., 2008. "Mechanical properties of longitudinal submerged arc welded steel pipes used for gas pipeline of offshore oil". Acta Metallurgica Sinica (English Letters), Vol. 21, n. 2, p. 85-93.

Zhao, Y., Ren, Q., Zou, T., Li, D. and Peng, Y., 2013. "Analysis and simulation of the UOE pipe production processing by finite element method". *Materials Science Forum*, Vol. 749, p. 437-443.

## 7. RESPONSIBILITY NOTICE

The authors are the only responsible for the printed material included in this paper.